70th International Astronautical Congress (IAC), Washington D.C, USA. 21-25 October 2019.

IAC-19, A7, 3, 9, x50660

A Low-Power CMOS Low Noise Amplifier for Space-based Low-frequency Radio Astronomy

Samaneh Babayan-Mashhadi [ab], Raj Thailak. Rajan [b], Mark Bentum [ac] , Chris Verhoeven [b]
[a] Eindhoven University of Technology, The Netherland,
s.babayan.mashhadi@tue.nl, m.j.bentum@tue.nl
[b] Delft University of Technology, The Netherlands,
s.babayanmashhadi@tudelft.nl, r.t.rajan@tudelft.nl, c.j.m.verhoeven@tudelft.nl
[c] ASTRON (Netherlands Institute for Radio Astronomy), The Netherlands
bentum@astron.nl

ABSTRACT

In modern radio astronomy, new science drivers have recently emerged for observation of low-frequency radio signals, below 30 MHz. Due to the atmospheric opacity and man-made interferers, exploring this frequency band requires a space-based radio telescope with a very large aperture that is impossible to realize in a monolithic fashion. Therefore, a distributed system consisting of a swarm of 50 or more nanosatellites is proposed in the OLFAR (orbiting low-frequency antennas for radio astronomy) project to realize such an instrument. Each of the OLFAR satellites will contain at least a single science antenna and subsequently the OLFAR array will comprise of a large number of receivers. In conventional radio telescopes, which typically consist of only a few receivers, expensive GaAs or InP cryogenically cooled HEMT transistors are used to implement the low-noise amplifier (LNA). HEMT transistors are capable of achieving excellent noise figures and have dominated the field of radio astronomy. However, due to the large number of nanosatellites used in OLFAR, less expensive, integrated nanometer CMOS technologies are more attractive to be used in LNAs implementations. Nevertheless, there exist many critical design challenges at low-frequencies which must be carefully considered such as the required signal-to-noise ratio (SNR), noise figure, linearity and area to be used in cube-satellites. In this paper, a novel CMOS-based integrated LNA is designed, analyzed and implemented to be used in the OLFAR project. The amplifier has 0.57 dB noise figure while consuming 0.2mW of power from a 1.8-V supply voltage and achieves output P1dB of -20dBm with the gain ranging from 34dB to 28dB across the OLFAR band (i.e., 0.3MHz-30MHz). The LNA represents one of the first CMOS designs that satisfies the very demanding requirements of low-frequency radio telescopes.

Keywords: OLFAR, space instrumentation, LNA Design

I. INTRODUCTION

Radio telescopes detect faint signals from celestial sources emitting electromagnetic radiation having wavelengths ranging from several meters to sub-millimetres [1]. The low-frequency radio astronomy that covers frequency ranges from 0.3MHz to 30MHz allows to obtain unique knowledge about exploration of the early cosmos during the dark ages, the discovery of planetary and solar bursts in other solar systems and the mapping of a tomographic view of the interstellar medium [2]. However, the Earth-based detection of astronomical long radio waves is severely hampered due to the atmospheric opacity and radio frequency interference (RFI). Hence, up to now, the frequency range below 30MHz remain one of the last unexplored frequency ranges in astronomy.

For this reason, several non-Earth-based telescopes have been proposed, some lunar based [3, 4] and some space based [5, 6]. The Orbiting Low Frequency Antenna for Radio Astronomy (OLFAR) [7] project is a feasibility study investigating a low frequency radio telescope in space using a swarm of autonomous Nano satellites. The satellites (approximately 50), will be spread over a virtual sphere with a diameter of 100km functioning as a single instrument.

The strength of the signal received by the radio telescope is very weak with typical values ranging from -150dBW m^{-2} to -220dBW m^{-2}. For instance, the strongest radio source at 300MHz has a power spectral density of about 10^5 Jansky (1 J = 10^{-26} Wm^{-2} Hz^{-1}). This requires the radio telescope receiver system to be more sensitive than other communication receivers by 50 to 60 dB [1].

The low noise amplifier (LNA) is a fundamental building block, whose performance in terms of noise figure, gain, bandwidth and power consumption, affects the overall performance of the radio telescope receiver and it is responsible for amplifying the weak received signal, and limiting the addition of extra noise. The device and technology which is used in the amplifier design, plays an important rule on the performance of the LNA and consequently the receiver. In [8], an LNA based on pHEMT transistors have been proposed to be used in Square Kilometer Array (SKA) project. HEMT transistors provide high gain and very low noise performance at high frequencies. However, they often require high voltages and have high harmonic contents which limit the linearity of the receiver. Recently, there has been great improvements in CMOS fabrication processes. While digital circuits benefit from technology scaling, analogue and mixed signal circuits face new design challenges to meet design requirements. In this project, an integrated circuit, low-power LNA in 0.18µm CMOS technology has been designed and is going to be fabricated. The design must be robust in different process corners and temperature variations.

There are some especial design considerations which should be carefully taken into account when designing space instrumentations. One of the important aspects is the effects of solar bursts which can saturate the system. Ionized particles such as alpha or beta can impact the devices and cause single event upsets or total ionization damage. Fig. 1, shows the flux noise spectra of the various celestial bodies and some radio emissions from the Earth along with background galactic noise over the frequency band [9]. As marked by dashed yellow lines, solar burst can be expected to be the strongest (around 10^{-14} Wm^{-2} Hz^{-1}). The dark black line is the galactic background noise, which is the "noise" observed in space environment. At frequencies lower than 1MHz, the QTN (Quasi Thermal Noise) dominates over sky noise, the combination of the two will be referred as sky noise throughout the paper for simplicity. For determining the sensitivity of the radio telescope, the receiver is said to be sky noise limited if its noise contribution is less than 1/10 of the sky noise. This value defines the maximum value for the noise figure that the receiver and consequently the LNA. Besides, the receiver should have large dynamic range to be able to observe both faint sky noise signals and also strong signals, without being saturated by large interfering signals. According to the values given in Fig. 1, the receiver must have minimum dynamic range of 70dB, which should be considered in the LNA design.

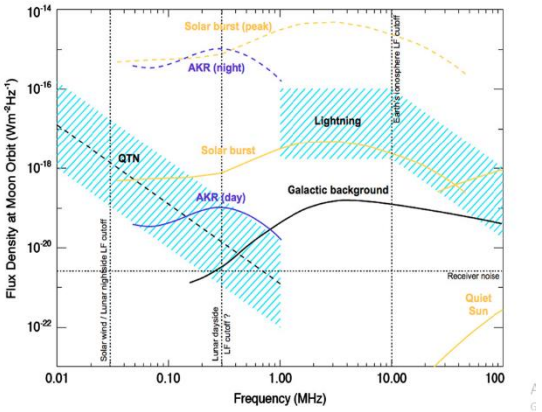

Fig. 1. Flux density spectra (in Wm^{-2} Hz^{-1}) of the noises plus radio emissions from the Earth (AKR-violet, and lightening –hatched blue) and the sun (yellow) [9]

Another aspect to consider in designing the LNA is the amount of Electromagnetic Interferences (EMI) that is generated by the satellite. Radiated emissions are due to the electronics (such as solar panels, power management system, etc.) radiating a field which couples to the antenna and other signal lines. In [10], a methodology followed to model the signals coupled into the analog signal path of the Netherlands-China Low-frequency Explorer (NCLE) due to the EMI produced by the Chengé-4 satellite is presented. It has been shown that the location of the NCLE antennas on the spacecraft influence not only the radiation performance of the antennas but also make it susceptible to interference produced by the spacecraft. Besides in [10], it has been shown that the interference levels at frequencies below 1 MHz pose the largest risk to drive the first stage amplifiers into saturation. In [10], in order to mitigate EMI, each analog channel on the LNA is designed to select between three frequency bands, limiting the instantaneous power at the input of the first amplification stage. Also using transformers at all antenna ports would help to isolate the spacecraft chassis, reducing the amount of EMI level.

Considering different design aspects, a table of requirement (Table. 1) has been made for the expected low-noise amplifier to be used in low-frequency space applications, particularly for the frequency band of interest in OLFAR project.

Table 1. LNA Design Requirements

Specifications	Values
Frequency Range	0.3-30 MHz
Temperature Range	-40° – 120° C
Dynamic Range	Min: 70dB , Max: 90dB
Noise	Max: 10^{-21} $Wm^{-2}Hz^{-1}$
Distortion Level	Max: 20 dB
Minimum Gain required	20dB
Power Consumption	<10mW

In this work, the analysis and design of a low-power gm-boosted, with shunt active feedback LNA is presented. The rest of the paper is organized as follows. In section II, the electrical model of the antenna is presented. Section III, presents the theory of a conventional resistive feedback trans-impedance amplifier (TIA) and noise analytical expressions are derived based on which, in Section IV, the new low-noise amplifier is presented and two proposed noise reduction techniques are discussed. In order to show the effectiveness of the proposed noise, reduction techniques, the proposed LNA is designed and simulated. The simulation results are demonstrated in section V, following by conclusion in Section VI.

II. ELECTRICAL MODEL OF THE ANTENNA

A critical component for the space-based array is the design of the observational antenna. A straightforward candidate for the observation antenna is a dipole antenna, which can be realized by rolling out metallic strips from the satellite. The observational wavelengths corresponding to the desired frequency range (i.e. 0.3MHz-30MHz) are much larger compared to the dimensions of the satellites and hence due to practical limitations, the realized dipole will be short compared to the wavelength (λ). A classic half-wave dipole for 10MHz and 30MHz observation frequencies yield a dipole length of 15m and 10m respectively.

For low frequencies, the radiation resistance (R_{rad}) of the small antenna would be low, resulting in less efficient antennas, as antenna radiation efficiency (η) and its resistances are defined as follows,

$$\eta = \frac{R_{rad}}{R_{rad} + R_{loss}}; \quad R_{rad} = 197 * \left(\frac{l}{\lambda}\right)^2; \; R_{loss} = \frac{l}{6\pi w}\sqrt{\frac{\pi f \mu}{2\sigma}} \quad (1)$$

In these equations, R_{rad} depends reversely on λ. R_{loss} refers to the ohmic loss of the antenna and depends on the dimensions of the antenna, its material and frequency of operation. Fig. 2 (a) (left figure) shows the radiation efficiency for a 10m tip-to-tip dipole antenna versus frequency. Besides, both antenna resistors (i.e., R_{rad} and R_{loss}) have been shown in Fig. 2 (a) (Right figure). It is evident that especially at low-frequencies, the radiation efficiency of antenna is decreased significantly, as R_{rad} goes lower than R_{loss}. This means the longer the antenna would be, the more efficiently it can receive the LF signals.

Up to now, in literature, many different electrical models have been presented for the dipole antennas [11-12]. In general, the impedance of the antenna can be modelled as a series combination of an R-L-C (Fig. 2(b)). R refers to the real part of the antenna impedance while L and C correspond to the equivalent imaginary part of the antenna impedance. CST simulations of a dipole antenna with 10m length results in C_{ant}=46pF, L_{ant}=4μH and R_{ant}=2KΩ. This values should be considered in LNA design. In case of using a transformer before LNA, the transferred Z_{ant} will be seen at the input of the LNA.

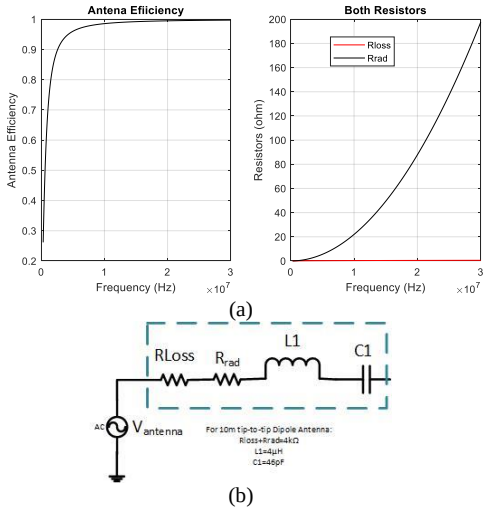

Fig. 2 (a) Antenna radiation efficiency, R_{loss} and R_{rad} versus frequency (b) electrical model of the antenna

III. Resistive Transimpedance Amplifier LNA Theory

Consider a simplified resistive transimpedance amplifier as shown in Fig. 3 (a). The model for the transimpedance noise analysis is shown in Fig. 3 (b). The operational amplifier is characterized by input-referred voltage noise of V_{nTIA} and current noise, $I_{n,opamp}$. In CMOS implementation, V_{nopamp} represents for flicker noise plus input-referred MOS channel thermal noise and the current noise represents gate-induced thermal noise, which increases with the frequency and is usually considerable for frequencies much higher than transistor transit frequency (f_T). Hence it can be neglected in OLFAR LNA design. The thermal noise produced by feedback resistor is modelled by, V_{nR} and appears directly in the output. Due to the feedback, the output noise of the TIA amplifier due to V_{nopamp} will be as follows,

$$V_{N,OUT} = V_{N,OPAMP}\left[\frac{A}{1+\beta A}\right] = V_{N,OPAMP}\,\frac{1}{\beta}\left[\frac{1}{1+\frac{1}{\beta A}}\right] \quad (2)$$

Where, β is the feedback factor and A is the open loop gain of the opamp, If βA >>1, then,

$$V_{N,OUT} = \frac{1}{\beta}V_{N,OPAMP} \quad (3)$$

For the circuit shown in Fig 2 (b), it can be shown that:

$$\frac{1}{\beta} = 1+\frac{R_f}{R_{ant}}.\frac{1+R_{ant}C_{ant}s}{1+R_fC_fs} \quad (4)$$

This may be rearranged to:

$$\frac{1}{\beta} = \left(\frac{R_{ant}+R_f}{R_{ant}}\right)\left[\frac{\tau_1 s+1}{\tau_2 s+1}\right]; \quad (5)$$

Where $\tau_1 = (R_f \parallel R_{ant})(C_{ant}+C_f)$ and $\tau_2 = R_fC_f$

Then, $f_1 = \frac{1}{2\pi\tau_1}$ and $f_2 = \frac{1}{2\pi\tau_2}$;

For very low frequencies ($f << f_1$), s approaches zero and Equation (2) will be:

$$V_{N,OUT} = \frac{1}{\beta}V_{N,OPAMP} = 1+\frac{R_f}{R_{ant}} \quad (6)$$

For very high frequencies ($f >> f_2$), this approaches infinity and Equation (2) becomes:

$$V_{N,OUT} = \frac{1}{\beta}V_{N,OPAMP} = 1+\frac{C_{ant}}{C_f} \quad (7)$$

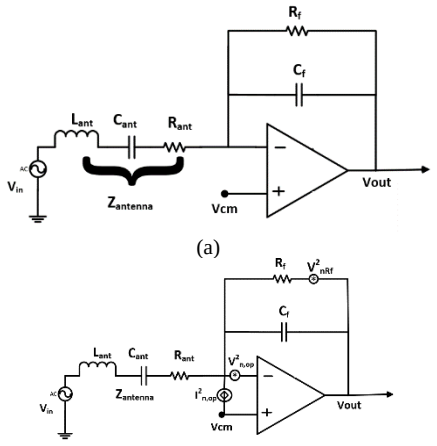

Fig. 3: (a) Resistive Transimpedance Amplifier (b) Noise model of the amplifier

Fig. 4 (a) shows the noise voltage gain and open loop gain of the opamp as function of frequency. The noise voltage spectral density at the output is obtained by multiplying the opamp's noise voltage spectral density times the circuit noise gain. Since both curves are plotted in log-log scales, the multiplication can be performed by the addition of the two curves (See Fig. 4(b)).

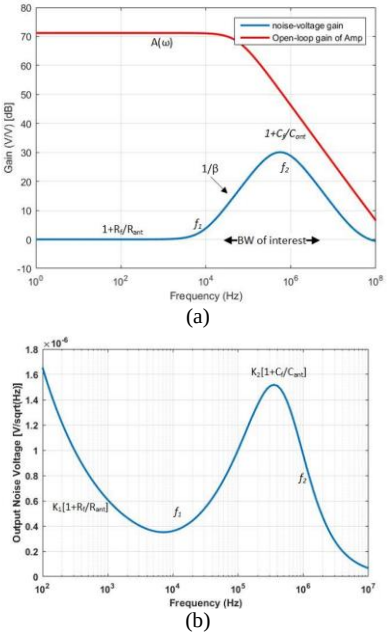

Fig.4. (a) Noise voltage gain (b) Output voltage noise spectral density

For a complete noise analysis of the circuit in Fig 2 (a), the noise of the feedback resistor, R_f, must also be included. The thermal noise of the resistor is given by:

$$V_{N,rms,Rf} = \sqrt{4kTR_f BW} \tag{8}$$

Where in this equation, *k* is the Boltzmann's constant, *T* is the absolute temperature (°K), R_f is the value of feedback resistor and *BW* is the operating bandwidth.

With R_f equal to 400kΩ, the RMS noise voltage, generated at the output will be about 0.44μV.

Finally, the total noise generated at the output due to the operational amplifier and resistive feedback will be as follows,

$$V_{Ntotal,OUT} = \sqrt{V_{n,out,opamp}^2 + V_{n,R_f}^2} \tag{9}$$

The presented noise analysis shows a trade-off between the DC gain of the resistive amplifier, its bandwidth and the noise performance of the whole amplifier as a function of R_f. Minimum R_f is beneficial from noise perspective, but it will degrade the DC gain and also shifts the bandwidth of the amplifier. In order to put the second pole of the amplifier on 30 MHz for OLFAR application, for reasonable value for C_f to be implemented on chip (i.e., few tens of pF), R_f in the order of 400kΩ is required which at the room temperature and 30MHz Bandwidth, generates 440μV RMS voltage noise. Considering the fact that the minimum sky noise received at the input is in the order of few μV, this amount of noise being generated by the trans-impedance amplifier is not acceptable. In the next section, it is shown how this issue can be solved using the proposed noise-reduction techniques.

III. PROPOSED LOW-NOISE AMPLIFIER

In the previous section, we came to the conclusion that R_f has significant effect, not only on the bandwidth of the amplifier and amplifier DC gain, but also it is one of the key contributors to the TIA noise voltage. Besides, the opamp noise voltage which is usually a function of flicker and thermal noise of input transistors, should be kept minimized. Thus, in order to meet OLFAR LNA requirements, and reduce the noise of the conventional TIA amplifiers, two different techniques have been proposed. Fig. 5, shows the schematic of the proposed low noise amplifier. The operational amplifier comprises two stages in a feedback loop. In order to maintain stability, miller compensation with series resistor has been used. First noise reduction technique, which has been applied is related to the use of active shunt feedback instead of using large R_f resistor (M_f in Fig. 5). The shunt transistor is biased in deep triode region, since its V_{DS}=0. In this bias point, the channel can be treated as a homogeneous resistor [13]. The noise in the channel is equal to:

$$i_{d,n}^2 = 4KTg_0 \quad [\text{A}^2/\text{Hz}] \tag{10}$$

where *k* is the Boltzman constant, *T* is the absolute temperature and g_0 is the channel conductance at zero drain-source voltage. For V_{GS} of 0.88, channel conductance (g_0) is equal to 1.98μA/V which results in, 38nV_{rms} noise output voltage (for R_L=50Ω and 30MHz bandwidth). Thus, not only a large resistive feedback can be implemented using an active transistor, but less noise voltage is produced in the output of the amplifier.

One important issue related with replacing passive components with active transistors, is that some of the transistors 'specifications such as threshold voltage, body-effect coefficient and in general, technology-dependent parameters vary depending on the fabrication. Thus, there is always a chance that with the fixed (W, L) transistor it shows different equivalent resistor or its parasitic capacitors, influence the feedback RC time-constant which affect TIA bandwidth. In order to see this effects, corner simulations have been done and fortunately with its applied gate voltage (V_{tune}), it is always possible to change the gate-source voltage of the transistor and

consequently its on-resistance will change. Also simulations show that since C_f is much higher than parasitic capacitors, the effect of parasitic capacitors on the bandwidth is less than 0.1 percent. This can also be calibrated with the V_{tune}.

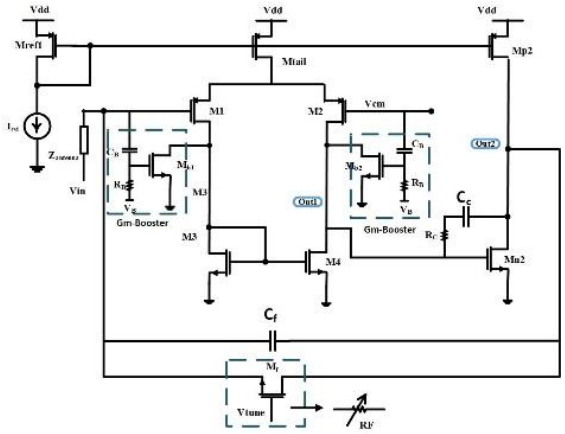

Fig. 5. The proposed noise reduction Gm-boosted LNA

The second noise reduction technique that has been applied in the LNA design is to use G_m-boosting technique on input transistors. It can be shown that without using G_m-boosting, the approximated input referred noise voltage of the opamp is obtained by,

$$v_{n,opamp}^2 = \frac{v_{n,out,opamp}^2}{A_v^2} = \frac{v_{n,flicker,M_{1,2}}^2 A_v^2 + 4kT\gamma g_{m1,2} R_{out1}.A_{v2}^{\ 2} + 4kT\gamma g_{mn2} R_{out2}}{(g_{m1,2} R_{out1}.g_{mn2} R_{out2})^2}$$

(11)

In this equation, g_{mi} refers to the transconductance of the M_i, $R_{out,I}$ is the output resistance of the i-th stage, *k* is the Boltzmann constant, T is temperature, γ is the thermal coefficient and $v_{n,flicker}^2$ is the spectral density of flicker noise of input transistors which appears directly at the input of the amplifier. It should be mentioned that in Equation (11), the noises related to the load transistors have been ignored for simplicity since their effect is highly reduced by the gain of the amplifier. Equation (11) indicates that the voltage noise power generated at the input is inversely proportional to the transconductance (g_m) of input transistors. In order to further reduce this noise power, G_m-boosting technique is applied via transistors M_{b1} and M_{b2}. Input voltage is also applied to these transistors, so the sum of $g_{m1,2}$ and $g_{mb1,2}$ will form the first-stage gain. Based on this, Equation (11) can be revised for G_m-boosted LNA as follows,

$$v_{n,opamp}^2 = \frac{(v_{n,flicker,M_{1,2}}^2 + v_{n,flicker,M_{1b1,b2}}^2)A_v^2 + 4kT\gamma(g_{m1,2} + g_{mb1,2})R_{out1}.A_{v2}^{\ 2} + 4kT\gamma g_{mn2} R_{out2}}{((g_{m1,2} + g_{mb1,2})R_{out1}.g_{mn2} R_{out2})^2}$$

(12)

As the effective G_m of the input transistors have been increased, the input-referred noise power is decreased. It should be noted that the addition of flicker noise of the added transistors (i.e. $M_{b1,2}$) in the input of the amplifier, does not degrade the noise performance, especially due to the fact that flicker noise does not appear in MHz frequency range of OLFAR. Next section will cover the simulation results which verify the proposed noise reduction techniques.

IV. SIMULATION RESULTS

The following Cadence simulation results were obtained using the TSMC 0.18µm CMOS technology. Fig. 6, shows the frequency response of the TI amplifier, for different values of shunt feedback time-constant. It can be seen that increasing the feedback capacitor, reduces the amplifier gain (since gain is set by the ratio of $C_{antenna}/C_f$). Besides, increasing the R_fC_f time-constant shifts the first pole to lower frequencies. In the proposed LNA, shunt resistor is implemented with an NMOS active device (V_{tune}=0.88V, w=10µm L=0.18µm and C_f=1pF) to meet the gain and bandwidth requirements. The parasitic capacitances of the active shunt feedback might affect the frequency bandwidth of the amplifier, so proper sizing of the active transistor and also the tuning voltage is important.

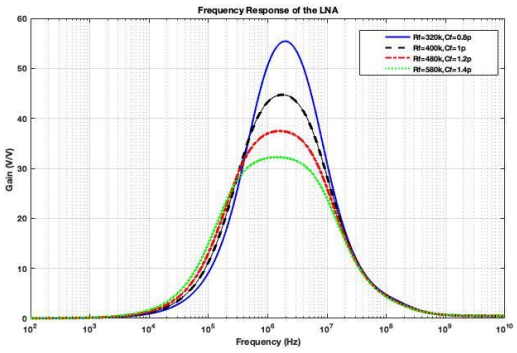

Fig. 6. Frequency response of the TI LNA for different shunt feedback time-constants (R_fC_f)

For simulating the noise performance of the TI LNA, noise contributions from both the passive and the active devices were considered in the simulation. Fig. 7, demonstrates the variation of the LNA noise figure (NF) across the frequency band of interest and for different working temperatures. For most of the frequency range, the NF is around 0.8 dB which meets the noise requirement. However, at high temperatures, NF is increased, although still fulfil the OLFAR requirements but it will limit the noise requirements on sub-blocks. It should be noted that usually in cubesat satellites, temperature is basically controlled to retain within standard range.

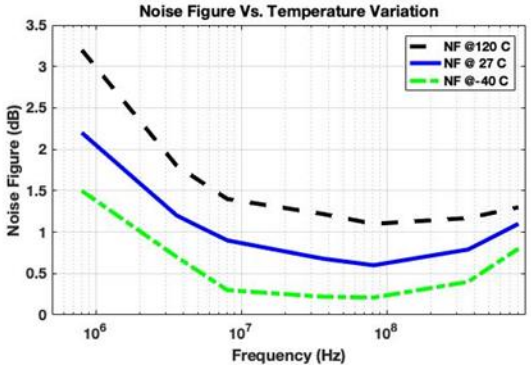

Fig. 7. Noise figure of the proposed LNA vs frequency

In order to demonstrate the effectiveness of the proposed noise reduction techniques (i.e., applying Gm-Boosting at input transistors and also using active shunt feedback instead of conventional resistor based TIA), both circuitries (proposed and the conventional TIA LNA with 400kΩ feedback resistor) have been simulated and evaluated. As illustrated in Fig. 8, the proposed noise-reduction techniques lead to significant reduction in the input-referred noise voltage of the TI amplifier.

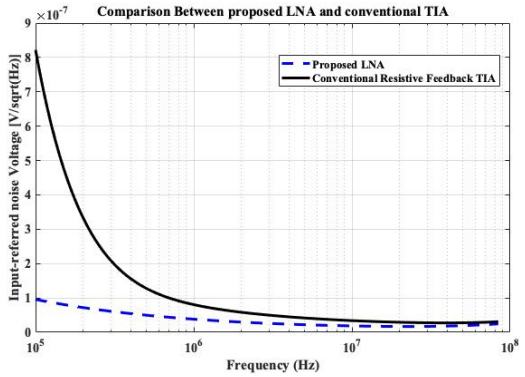

Fig. 8. Input-referred noise voltage of the amplifier with/without proposed noise-reduction techniques.

Finally, Table I summarizes the simulation results of the designed LNA and compares it to the simulated performance of another low frequency band SKA LNA implemented in a pHEMT technology. The proposed LNA exhibits a good performance, while being implemented in a cheaper CMOS technology.

Table 2. Comparison of single-ended recent LNAs

Reference	[8]	[9]	**This Work**
Technology (µm)	pHEMT	0.18	0.18
Supply Voltage (V)	1	1.5	1.8
Frequency (MHz)	70-450	50-350	0.3-30
Gain (dB)	38	38	34
Power Consumption(W)	72mW	72mW	0.2mW
NFmin at room temp (dB)	0.2	0.32	0.6
IP-1dB (dBm)	-	-18	-20

V. CONCLUSION

The design and analysis of a 0.18µm CMOS low noise amplifier for low-frequency space instrumentation has been presented. The proposed LNA exhibits a forward gain of more than 30dB over the entire bandwidth with the maximum value of 38dB, while consuming only 0.2mW from 1.8V supply voltage. The bandwidth of the amplifier is designed based on OLFAR project requirements. The minimum NF of 0.57dB is obtained at room temperature. Process corner simulations also guarantee proper operations of the proposed LNA in different process and temperature corners.

REFRENCES

[1] J. M. Ford K. D. Buch "RFI mitigation techniques in radio astronomy", Proc. IEEE Int. Geosci. Remote Sens. Symp. (IGARSS) pp. 231-234 Jul. 2014.

[2] D. M. P. -Smith M. J. Arts A.-J. Boonstra and S. J. Wijnholds "Characterisation of astronomical antenna for space based low frequency radio telescope " in Aerospace Conference, IEEE Big Sky MT, pp. 1-9, March 2013.

[3] S. J. Wijnholds and J. D. Bregman, “Design concept for a lunar low frequency array,” ASTRON, Dwingeloo, Tech. Rep. RP–160, Apr 2007.

[4] C. L. Carilli, J. N. Hewitt, and A. Loeb, “Low frequency radio astronomy from the moon:

Cosmic reionization and more," in Astrophysics Enabled by the Return to the Moon, Baltimore, pp. 1–15, 28–30 Nov 2007.

[5] W. A. Baan, "Space-based ultra-long wavelength radio observatory," ASTRON, Dwingeloo, Proposal for ESA's Cosmic Vision 057, Dec 2010.

[6] A. J. Boonstra, M. J. Bentum, R. T. Rajan, S. J. Wijnholds, W. van Cappellen, N. Saks, H. Falcke, and M. Klein-Wolt, "DARIS: Distributed aperture array for radio astronomy in space," ASTRON, Dwingeloo, Final Report 22108/08/NL/ST, Mar 2011.

[7] M. J. Bentum, C. J. M. Verhoeven, and A. J. Boonstra, "OLFAR – orbiting low frequency antennas for radio astronomy," in Annual Workshop on Circuits, Systems and Signal Processing, Veldhoven, pp. 1–6, 26–27 Nov 2009.

[8] M. Panahi, "Lna considerations for square kilometre array," Ph.D. dissertation, School of Electrical and Electronic Engineering, Manchester, UK: The University of Manchester, 2012.

[9] P. Zarka, J. L. Bougeret, et al., "Planetary and explanetary low frequency radio observations from the moon", In: *Planetary and Space Science*, vol. 74, issue 1, pp. 156-166, 2012.

[10] D. Prinsloo, M. Ruiter et. al., "EMI Modeling of an 80kHz to 80MHz Wideband Antenna and Low-Noise Amplifier for Radio Astronomy in Space,", 12th *European Conference on Antennas and Propagation* (EuCAP 2018), pp.461-465, 2018.

[11] W. O. Coburn and C. Fazi, "A Lumped-Circuit Model for a Triband Trapped Dipole Array-Part 1: Model Description," *in IEEE Antennas and Wireless Propagation Letters*, vol. 8, pp. 14-18, 2009.

[12] O. O. Olaode, W. D. Palmer and W. T. Joines, "Characterization of Meander Dipole Antennas With a Geometry-Based, Frequency-Independent Lumped Element Model," in *IEEE Antennas and Wireless Propagation Letters*, vol. 11, pp. 346-349, 2012.

[13] Laker, K. R. and Willy Sansen. "Design of analog integrated circuits and systems." McGraw-Hill Education, (1994).